A Desktop Model for Computing Acceleration Severity Index (ASI) for Rigid Barrier Impacts as a Function of Impact Configuration

Andrew Burbridge[a,b] and Rod Troutbeck[b]

[a]Queensland Department of Transport and Main Roads, [b]CARRS-Q, Queensland University of Technology

Abstract

Acceleration Severity Index (ASI) is a vehicle occupant severity indicator measured during homologation of road safety barriers. Published literature contains efforts to correlate occupant injury risk with ASI. Hence there is value in exploring how ASI might vary with impact configuration (impacting vehicle mass, speed and angle). This paper describes the development and testing of a desktop model for predicting ASI in impacts with rigid barriers as a function of impact configuration. The efficacy of the model is discussed and tested against published data.

Introduction

Acceleration Severity Index (ASI) is a non-dimensional vehicle occupant severity indicator calculated from orthogonal time-averaged time-acceleration traces measured during crash testing at the centre of mass of the impacting vehicle. ASI is calculated using Equation 1:

$$\text{ASI} = \max\left[\left(\frac{a_x}{\hat{a}_x}\right)^2 + \left(\frac{a_y}{\hat{a}_y}\right)^2 + \left(\frac{a_z}{\hat{a}_z}\right)^2\right]^{\frac{1}{2}} \qquad \text{Equation 1}$$

where $a_{x,y,z}$ are average component vehicle accelerations respectively in the longitudinal, lateral and vertical direction measured over a prescribed time interval (50 milliseconds), and $\hat{a}_{x,y,z}$ are corresponding threshold values for the respective component accelerations (Gabauer & Gabler, 2005). The denominator values for the component threshold accelerations $\hat{a}_{x,y,z}$ as adopted in both the US and European test protocols (AASHTO, 2009; European Committee for Standardization, 2010a) are respectively $\hat{a}_x = 12\text{g}$, $\hat{a}_y = 9\text{g}$ and $\hat{a}_z = 10\text{g}$ (g = acceleration due to gravity).

The appeal of ASI as a comparative metric is that it is required to be reported for longitudinal road safety barriers under European Normative EN1317 (European Committee for Standardization, 2010a, 2010b), and while reporting of ASI is not required under US test protocols MASH (AASHTO, 2009) or NCHRP Report 350 (Ross et al., 1993) it is required to be reported under Australian/New Zealand Standard AS/NZS 3845.1-2015 (Standards Australia, 2015).

The relevance of ASI is evident in published literature, which contains efforts to correlate occupant injury risk with ASI (Li et al., 2015; Roque & Cardoso, 2013; Shojaati, 2003). Gabauer and Gabler (2005) describe efforts to correlate ASI directly with occupant injury, finding that "*ASI, at least with respect to the preferred threshold, is a good indicator of (minor levels of) occupant injury to belted and airbag-restrained occupants involved in frontal collisions*". Sturt and Fell (2009) report on the results of three physical crash tests with validating simulations and 47 other simulations, in which a small car is impacted into concrete "step" profile barrier with impact speeds ranging between 109 km/h and 113 km/h, and impact angles ranging between 15° and 20°. They report among other things a correlation between head and neck injury and ASI, with ASI=2.0 considered to be the threshold for unacceptable injury. The point here is that vehicle occupant injury appears to be positively correlated with ASI.

Burbridge and Troutbeck (2017a) report on the results from full-scale crash tests into a range of road safety barriers, and conclude, among other things, that occupant risk measured in terms of ASI is likely to be a function of the speed, mass and angle of the impact as well as the flexibility of the barrier system. So for similar impact configurations (mass, speed and angle), ASI should be higher for the stiffer system and lower for the more flexible system. Burbridge and Troutbeck (2017b) present the basis for a "structural" model explaining how occupant trauma disutility arising from road safety barrier impacts might be predicted via the proxy of ASI if the impact configuration and barrier system stiffness are known.

Subsequent review and analysis of the data (with slight amendment) reported by Burbridge and Troutbeck (2017a) suggests that the relationship between barrier flexibility and the reciprocal of ASI (1/ASI) is a linear function, and that the shape (y-intercept and slope) of the linear function is a function of impacting vehicle mass, speed and angle. See Figure 1. Similar relationships (also depicted at Figure 1) are evident in re-analysis of parametric crash testing reported by Hammonds and Troutbeck (2012), and in analysis of data reported by Anghileri et al (2005). In summary, it is conjectured that:

$$\frac{1}{ASI} = a\frac{DD}{IS} + b \qquad \text{Equation 2}$$

and thus:

$$ASI = \frac{1}{a\frac{DD}{IS} + b} \qquad \text{Equation 3}$$

where 'a' is the slope of the proportional relationship between 1/ASI and flexibility, while 'b' is the y-intercept, DD is the dynamic deflection (m) and IS is impact severity (kJ) computed via the expression at Equation 4.

$$IS = \frac{1}{2}m(v.sin\,\theta)^2 \qquad \text{Equation 4}$$

where m is the mass of the impacting vehicle (t), v is impact speed (m/s) and θ is impact angle. So for rigid barriers (where dynamic deflection is zero):

$$ASI_{rigid} = \frac{1}{b} \qquad \text{Equation 5}$$

Ideally, given that ASI is effectively a measure of resultant (albeit weighted) acceleration, it would be preferable in a structural explanatory model to compute ASI from predictions of impact loads, for example as proposed by Jiang et al. (2004). However while this methodology may be useful for predicting peak loads for purposes of the structural integrity of the barrier itself, its application to computing ASI, which is based on 50 millisecond average accelerations has not been demonstrated. This is depicted quite well in information presented by Noel et al. (1981), whereas instrumented wall studies generally report peak loads (eg Hirsch et al. (1989)). Moreover, as described by (for example) Jehu and Prisk (1967) the deceleration force acting on an impacting vehicle might be considered as the resultant of a component force normal to the plane of the barrier and a parallel frictional component, so it would still be necessary without a measured value to "assume" a friction coefficient. This is unfortunate, in the sense that an explanatory structural equation must be preferred over an equation deduced by regression. However in the absence of such an explanatory structural equation, the hypothesis here is that the denominator 'b' term is a function of vehicle mass (m), impact speed (v) and angle (θ), such that:

$$b = K_b m^{\alpha_b} v^{\beta_b} (sin\,\theta)^{\gamma_b} \qquad \text{Equation 6}$$

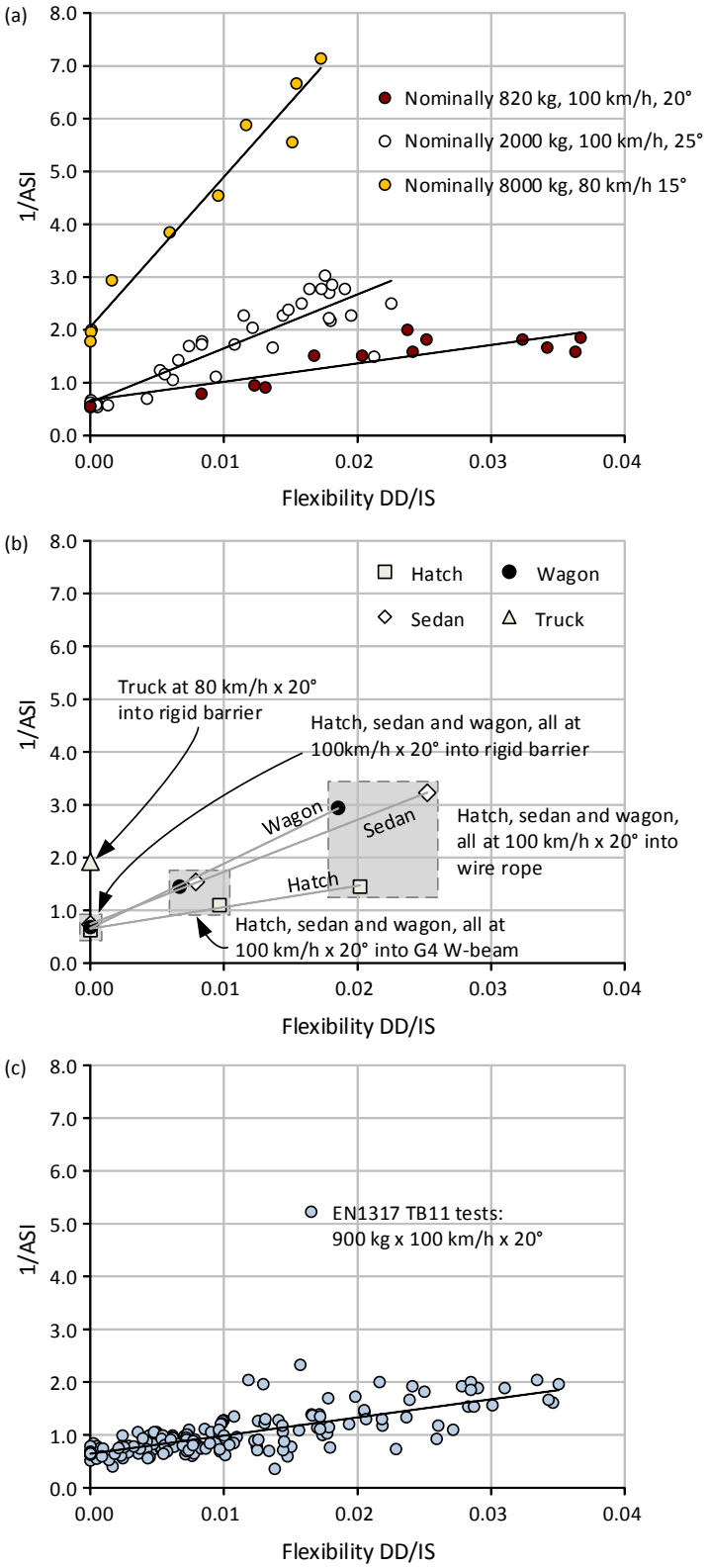

Figure 1 (a) Analysis of data from Burbridge and Troutbeck (2017a), (b) 1/ASI v flexibility plot using data from crash testing reported by Hammonds and Troutbeck (2012), and (c) 1/ASI v flexibility plot of 174 no. EN1317 TB11 test results from Anghileri et al (2005).

and thus: $$ASI_{rigid} = \frac{1}{K_b m^{\alpha_b} v^{\beta_b} (sin\,\theta)^{\gamma_b}}$$ Equation 7

for rigid barrier impacts, where K_b, α_b, β_b and γ_b are constants, which can then be simplified to:

$$ASI_{rigid} = K_b' m^{\alpha_b'} v^{\beta_b'} (\sin\theta)^{\gamma_b'}$$ Equation 8

The broad aims of this study are to construct and then test a desktop model that predicts ASI values for impacts into rigid barriers according to the expression in Equation 8. The specific objectives are to determine values for $K_b', \alpha_b', \beta_b'$ and γ_b' and to critique the resulting function.

Method

A least sum of the squared differences (SSD) regression was undertaken using results from 47 full scale impacts into barriers where impacting vehicle mass, speed, angle, ASI and zero dynamic deflection are reported in order to determine 'best-fit' values for $K_b', \alpha_b', \beta_b'$ and γ_b'***. The base data is provided here at***

Table 1.

The residual error RE_i is the difference between the value of ASI observed in the i^{th} test and the value for ASI predicted by Equation 9 for the same i^{th} impact configuration.

$$ASI_{obs,i} - ASI_{pred,i} = RE_i$$ Equation 9

The least sum of squares of differences seeks to find values of $K_b', \alpha_b', \beta_b'$ and γ_b' such that the residual sum of squares (RSS in Equation 10) is minimised. This was undertaken using the <solver> function in Microsoft Excel.

$$RSS = \sum_{i=1}^{47} (RE_i)^2$$ Equation 10

Table 1 Observed data from full scale testing

Type	Test ref.	Test type	Mass (kg)	Speed (km/h)	Angle (deg)	ASI	Source
Steel	TTI 404311-1	3-10	820	100.0	20.8	1.80	Buth, Williams, Menges, et al. (1998)
Concrete	TTI 418048-4	3-10	820	100.7	20.3	1.57	Buth, Williams, Bligh, et al. (1998)
Concrete	TTI 418048-1	3-11	2000	101.3	24.9	1.40	Buth, Bligh, et al. (1998)
Steel	TTI 404531-1	3-10	820	99.9	19.1	1.62	Buth et al. (1999)
Concrete	TTI 408460-1	3-11	2000	101.6	25.5	1.78	Bullard et al. (2001)
Concrete	TTI 408460-2	4-12	8000	83.4	14.9	0.72	Bullard, et al. (2001)
Stone	TTI 400001-SCW1	3-11	2000	101.6	25.2	1.60	FHWA (2000)
Concrete	TTI 442882-1	3-11	2044	98.8	24.8	1.50	Bullard et al. (2002)
Concrete	TTI 442882-2	3-11	2052	101.1	26.1	1.76	Bullard, et al. (2002)
Concrete	TTI 442882-4	3-10	820	99.1	20.4	1.79	Bullard, et al. (2002)
Concrete	TTI 441382-1	3-11	2042	101.0	26.1	1.49	Buth et al. (2002)
Concrete	TTI 441382-2	3-11	2044	100.7	25.0	1.62	Buth, et al. (2002)
Concrete	CA_DOT_581	3-10	823	97.7	20.0	1.65	Speer et al. (2002)

Type	Test ref.	Test type	Mass (kg)	Speed (km/h)	Angle (deg)	ASI	Source
Concrete	CA_DOT_582	3-10	801.5	96.7	20.0	1.40	Speer, et al. (2002)
Concrete	CA_DOT_583	3-11	1992	100.2	25.0	1.55	Speer, et al. (2002)
Concrete	CA_DOT_584	3-10	842	95.8	19.3	1.62	Speer, et al. (2002)
Concrete	CA_DOT_585	3-11	1958	99.2	24.3	1.97	Speer, et al. (2002)
Concrete	CA_DOT_587	3-11	2027	101.1	23.6	1.68	Speer, et al. (2002)
Concrete	CA_DOT_588	3-11	1965	100.3	24.0	2.15	Speer, et al. (2002)
Concrete	CA_DOT_589	3-11	1956	100.8	23.6	1.77	Speer, et al. (2002)
Concrete	TTI 421323-1	4-12	8009	81.4	14.3	0.56	Alberson, Williams, et al. (2004)
Concrete	TTI 421324-3	4-12	8068	80.5	16.8	0.69	Alberson, Menges, et al. (2004)
Unknown	Robust D.2.1_#38	TB11	900	100.8	20.0	1.57	Anghileri, et al. (2005)
Unknown	Robust D.2.1_#43	TB11	900	101.0	19.9	1.94	Anghileri, et al. (2005)
Unknown	Robust D.2.1_#46	TB11	900	101.2	20.0	1.44	Anghileri, et al. (2005)
Unknown	Robust D.2.1_#54	TB11	900	101.4	20.0	1.53	Anghileri, et al. (2005)
Unknown	Robust D.2.1_#104	TB11	900	102.7	20.0	1.27	Anghileri, et al. (2005)
Unknown	Robust D.2.1_#110	TB11	900	102.8	20.0	1.46	Anghileri, et al. (2005)
Unknown	Robust D.2.1_#115	TB11	900	103.0	20.0	1.57	Anghileri, et al. (2005)
Unknown	Robust D.2.1_#124	TB11	900	103.2	20.0	1.59	Anghileri, et al. (2005)
Unknown	Robust D.2.1_#130	TB11	900	103.4	20.0	1.57	Anghileri, et al. (2005)
Unknown	Robust D.2.1_#132	TB11	900	103.5	20.0	1.50	Anghileri, et al. (2005)
Unknown	Robust D.2.1_#139	TB11	900	103.8	20.0	1.59	Anghileri, et al. (2005)
Unknown	Robust D.2.1_#143	TB11	900	104.0	20.0	1.54	Anghileri, et al. (2005)
Concrete	LIER_Rou664	TB11	862	100.4	20.0	1.90	LIER (2006)
Concrete	Autostrade_S70	TB11	922	100.3	20.0	1.60	LIER (2006)
Concrete	CIDAUT_00B112002	TB11	902	101.4	20.5	1.70	LIER (2006)
Concrete	TRL_13NB	TB11	935	102.8	20.4	1.90	LIER (2006)
Concrete	LIER_ROB981	TB11	903	100.9	20.0	1.87	LIER (2006)
Concrete	TRL_B3089	TB11	916	103.2	20.0	1.80	LIER (2006)
Composite	CA_DOT_632	3-10	789	76.5	19.5	1.18	Whitesel et al. (2008)
Composite	CA_DOT_633	3-10	810	99.2	20.0	1.70	Whitesel, et al. (2008)
Concrete	TTI 420020-3	3-11	2284	102.7	24.8	2.02	Williams et al. (2011)
Concrete	BR2010-006	-	841	99.0	19.6	1.60	Sherry and Jackson (2010a)
Concrete	BR2010-010	-	1597	99.0	20.5	1.37	Sherry and Jackson (2010b)
Concrete	BR2010-011	-	2269	98.8	20.5	1.47	Sherry and Jackson (2010c)
Concrete	BR2010-013	-	7989	80.5	19.8	0.52	Sherry and Jackson (2010d)

Analysis of the results includes correspondence plotting and cumulative residual (CURE) graphs (Hauer, 2015) for each independent variable.

The model was then used to predict values for ASI for various impact configurations, which were subsequently compared with values generated in corresponding parametric simulations conducted earlier by Montella and Pernetti (2004).

Results

The <solver> function in Microsoft Excel was run repeatedly, iteratively varying values of independent variables to return the lowest value of RSS. Substituting these ‘best fit’ values back into Equation 6 gives Equation 11. Post hoc review of the trial results suggested that the ‘best fit’ model could be rationalised (Equation 12) by simplifying the exponents without detriment to the

results. Sets of parameters from both the least SSD solution and the rationalised model are tabulated in Table 2.

$$ASI_{rigid} = \frac{0.104602 \times v^{1.135923} \times (sin\,\theta)^{0.991787}}{(m/1000)^{0.200600}} \quad \text{Equation 11}$$

$$ASI_{rigid} = \frac{0.165744.\, v.\, (sin\,\theta)}{(m/1000)^{0.2}} \quad \text{Equation 12}$$

Table 2 Results of regression

Variable		Least SSD model	Rationalised model
Constant	K'	0.104602	0.165744
Mass	α'	-0.200600	-0.2
Speed	β'	1.135923	1
Angle	γ'	0.991787	1
SSD		1.5903	1.5949
Maximum residual (high)		0.39	0.38
Maximum residual (low)		-0.51	-0.51
R^2		0.7090	0.7099

Table 3 Analysis of variance table: Least SSD model

Source of variation	DF	SS	Mean Sq.	F_{fit}
MSR (model)	4	3.8913	0.97281	26.30
MSE (error)	43	1.5903	0.03698	
Total	47	5.4816		

Table 4 Analysis of variance table: Rationalised model

Source of variation	DF	SS	Mean Sq.	F_{fit}
MSR (model)	4	3.8867	0.97167	26.20
MSE (error)	43	1.5949	0.03709	
Total	47	5.4816		

The rationalised solution is a 'nested' model of the more complex solution. Analysis of variance tables are provided for both models at Table 3 and Table 4. The rationalised model is shown to be statistically significant at the α=0.05 level: $F_{fit} = 26.20 > F_{crit}(4, 43, 0.05) = 2.59$ ($p<0.001$). There is (as might be expected) observed to be some degradation of the model (e.g., comparing R^2: 0.7099>0.7090), but the quantum is not substantial, subjectively at least. The question is whether, statistically, the models are not different. This is tested here with a one-tailed test of the ratio of the mean squares. Since the ratio $0.03709/0.03698 = 1.0029 < F_{crit}(43, 43, 0.05) = 1.6607$ ($p=0.4963$), there is insufficient evidence to reject the hypothesis that the models are not different. As such, the simpler model can be adopted. In this paper, the subsequent analysis is of the results obtained using the rationalised model (Equation 12).

Using Equation 12, ASI is computed for the mass, speed and angle configuration reported in each crash test. Observed versus predicted values of ASI and distribution of residuals (Equation 9) are shown in Figure 2. It is observable that the data are distributed *somewhat* around the y=x line, with 40 of the 47 results (85.1%) within ±0.3. The plot highlights a shortcoming of the data, which is that the observed data are in two distinct clusters. The absence of any data between and beyond these clusters is problematic because the basis of the model is not necessarily representative either in-

between or beyond the range of the empirical data. This raises concern about the "independence" of the three independent variables: mass, speed and angle. For example, all 2000 kg nominal vehicle mass tests are conducted at nominally 100 km/h and 25 degrees, while all four 8000 kg nominal vehicle mass tests are conducted at nominally 100 km/h.

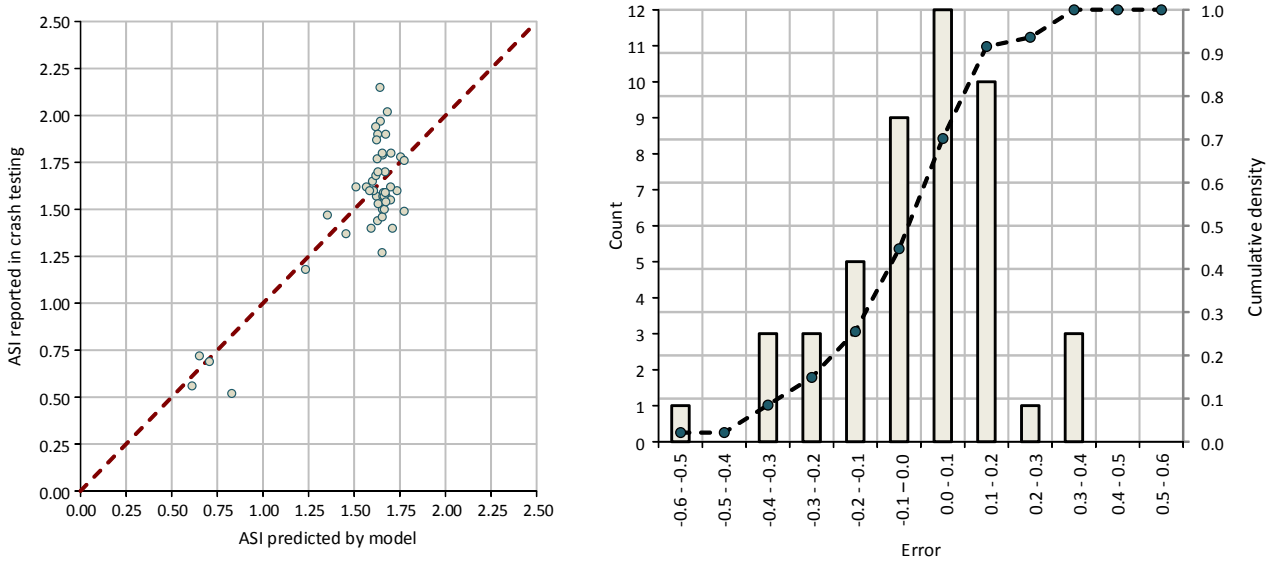

Figure 2 (left) Correspondence plot showing observed (reported) ASI v ASI predicted by Equation 12, and (right) distribution of residuals (indicating normal distribution).

The difference between observed and predicted values ranges from -0.51 to +0.38 (see histogram at Figure 2), which might (fairly) be regarded as substantial. A reasonable question is whether this can be ascribed to a flaw in the model. 41 of the 47 tests represent four test configurations. Table 5 and Figure 3 present maximum, minimum and average values observed from tests of the same nominal configuration. In general, the average observed value for each nominal test configuration resides on the y=x line (Figure 3), suggesting that the model has some level of validity, at least for the predominant test configurations present in the data. Of note the single MASH 3-11 test result is an under-prediction (observed = 2.02, predicted = 1.65). This difference may be attributable to the model under-predicting or the observed result being unusually high, or some combination of those reasons. Alternatively, there may be an argument that the MASH 3-11 standard test vehicle is stiffer than the NCHRP Report 350 standard test vehicle. In order to investigate this further a larger data set of MASH 3-11 test results of impacts into rigid barriers is required.

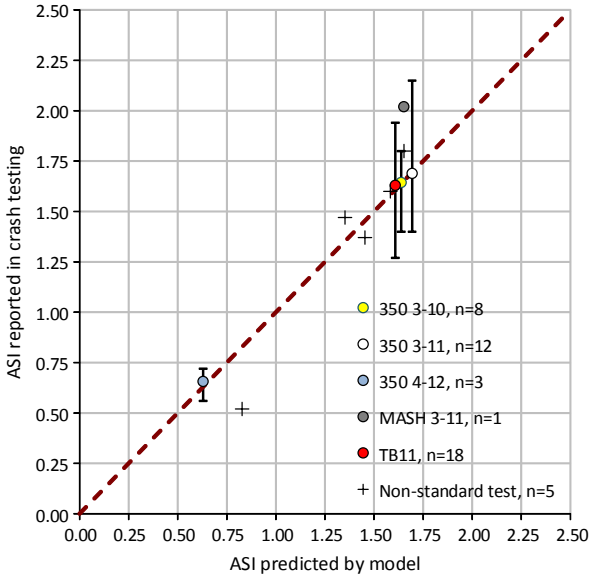

Figure 3 Comparison of predicted values of ASI for each nominal test configuration with maximum, minimum and average values observed from tests of the same configuration.

Table 5 Comparison of predicted values of ASI for each nominal test configuration with maximum, minimum and average values observed from tests of the same configuration

Test	Count	ASI_predicted	ASI_ave_obs	ASI_max_obs	ASI_min_obs
350 3-10	8	**1.64**	**1.64**	1.80	1.40
TB11	18	**1.61**	**1.63**	1.94	1.27
350 3-11	12	**1.69**	**1.69**	2.15	1.40
350 4-12	3	**0.63**	**0.66**	0.72	0.56

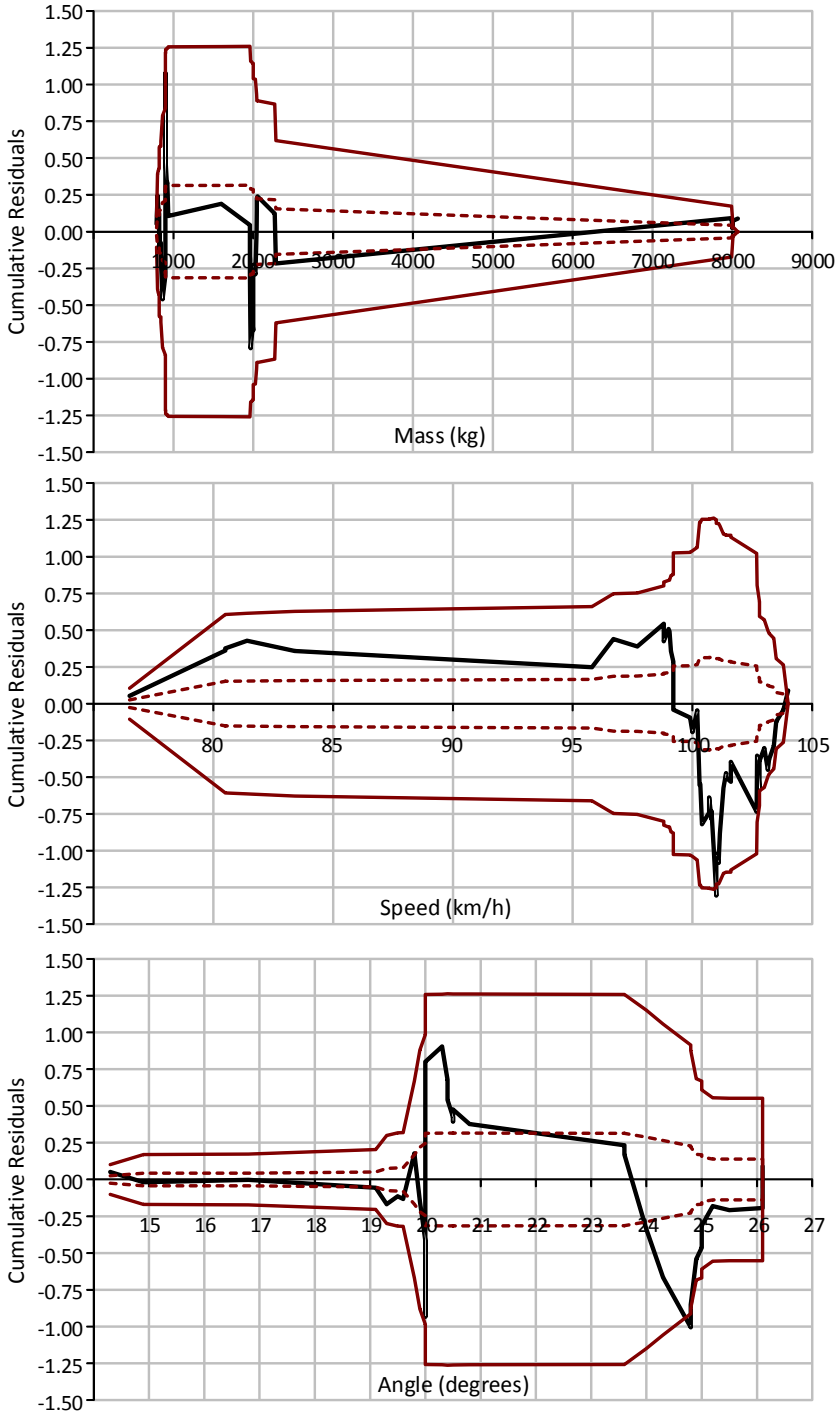

Figure 4 Plots of cumulative residuals (CURE) v each independent variable (ranked in ascending order) (Hauer, 2015): mass (top), speed (middle) and angle (bottom). The dashed and solid red envelopes respectively represent a half standard deviation and two standard deviations of the cumulative residuals.

Cumulative residual (CURE) plots for each independent variable are provided at Figure 4. In each plot, the black line represents the magnitude of the cumulative sum of residual errors plotted against the respective independent variable ranked in ascending order, while the dashed and solid red envelopes respectively represent a half standard deviation and two standard deviations of the cumulative residuals. In the case of each independent variable (mass, speed and angle), the residual plot is prone to perturbations at the values corresponding with the standardised test configurations, but is generally flat/even in between due to the absence of data. Similar 'striping' is evident in bivariate plots of residual against each independent variable (not depicted here). Nevertheless, the

data can be regarded as generally well behaved, rarely breaching the two standard-deviation envelope.

Finally, Montella and Pernetti publish ASI predicted by simulation for two vehicle masses (900 kg and 1500 kg) impacting a rigid barrier at five impacts speeds (50, 80, 100, 130 and 150 km/h) and six impact angles (2.5, 7.5, 12.5, 20, 25 and 30 degrees). Comparison of ASI values derived using Equation 12 for impact conditions corresponding to those used by Montella and Pernetti (2004) for simulation are presented in Figure 5. Visual analysis of the plotted data suggests that the model is generally under-predicting compared to the simulated results. This is discussed further in the discussion below.

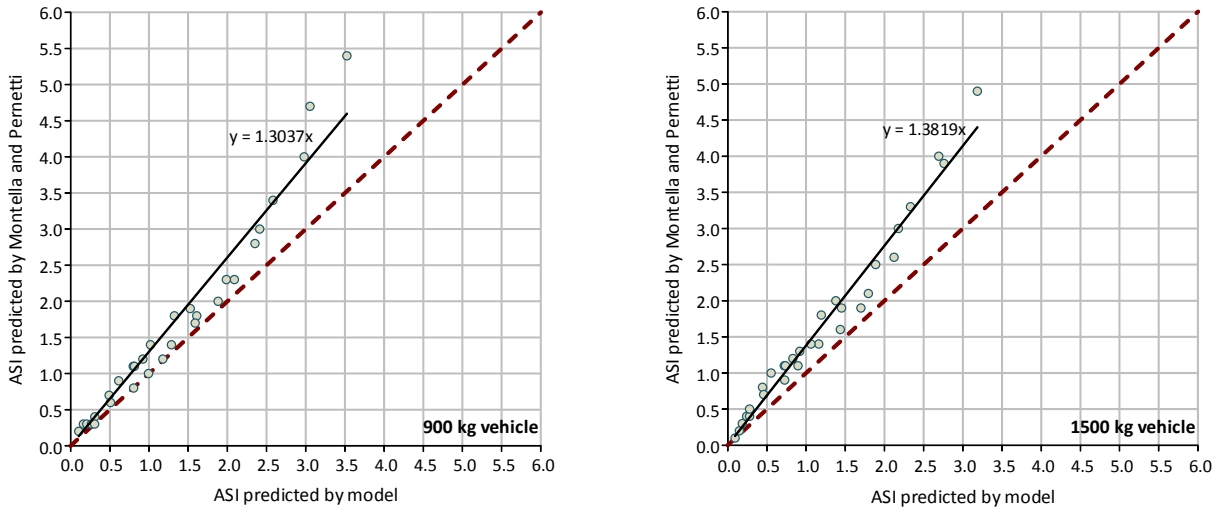

Figure 5 Comparison with simulated results predicted by Montella and Pernetti (2004)

Discussion

In summary, the model has demonstrated some level of validity (Figure 3), but would be expected to benefit from further refinement, ideally based on the results from full scale crash testing in configurations that are different from the standardised configurations that are prescribed in the test protocols. This limitation of the model is evident in both the correspondence plot at Figure 2 and the CURE plots at Figure 4.

In terms of speed, it is observed that 42 of the 47 data points are at speeds 100±5 km/h, which raises questions about the usefulness of the speed CURE plot. The plot indicates some level of over-prediction at ~80-100 km/h which is then compensated with under-predictions at >100 km/h. In terms of impact angle, the single breach of the two standard-deviation envelope of the angle CURE plot is the result of six successive model under-predictions, four of which correspond to ASI values for NCHRP Report 350 3-11 tests conducted on textured concrete wall reported by Speer, et al. (2002). While this could be interpreted as significant, the fifth NCHRP Report 350 3-11 test result reported by Speer, et al. (2002) is lower than that predicted by the model. This apparent bias in the model is exacerbated by the second largest recorded under-prediction, which is reported against the single MASH 3-11 test result in the data set (from Williams, et al. (2011)).

In terms of mass, this same result (from Williams, et al. (2011)) is adjacent (when ranked by ascending mass) to an under-prediction for the 2269 kg test reported by Sherry and Jackson (2010c). Here, it is necessary to observe that the test vehicle in the test reported by Sherry and Jackson was a 1998 Toyota Landcruiser (impacting at 20 degrees), and not a MASH test vehicle.

At the lighter end of the vehicle spectrum, standardised test configurations conducted with vehicles with nominal masses 820 kg and 900 kg are otherwise nominally similar (100 km/h at 20 degrees),

meaning that mass is the only explanatory variable in the model. The model returns a cumulative residual from the eight nominal NCHRP Report 350 3-10 tests of -0.23, and a cumulative residual from 18 nominal EN 1317 TB11 tests of +0.29. Since there is no obvious reason why this might be so, it may be (as indicated by Naish and Burbridge (2015)) that ASI is calculated differently according to different test protocols.

Further, twelve EN 1317 TB11 data points reported by Anghileri, et al. (2005) are from nominally identical tests yet represent ASI values ranging from 1.27-1.94, whereas the model predicts a much narrower range of 1.62-1.67. The test mass is unreported by Anghileri, et al. (2005) and is assumed to be the nominal test mass (900 kg). However speed and angle are reported, and range, respectively, from 100.8 to 104.0 km/h and from 19.9 to 20.0 degrees. Anghileri (2003) reports for example that variations in car details, tyre condition, data acquisition (transducers, mounting), and methods of data filtering and evaluation may be responsible for "remarkable scatter", none of which are accounted for in this model.

Finally, aside from possible variations in test vehicle, the model does not take into account variations in the barrier itself. Naish and Burbridge (2015) (for example) observed that different barrier profiles may be responsible for variation in ASI outcomes. Moreover the material of the face of the barrier may be responsible for different effective friction. The data set used in this study is known to contain examples of steel systems and of concrete barriers of various shape and surface profile, none of which is accounted for in the model.

Comparison with Montella and Pernetti

It was observed that visual analysis of the plotted data indicates that the model is generally under-predicting compared to the simulated results presented by Montella and Pernetti (2004) (Figure 5). It is noted however that Montella and Pernetti do not present a true validation of their model, but do present a comparison with one result (ASI = 1.9) reported to be from round robin testing the European Normative EN1317-2 TB-11 test configuration, i.e., a 900 kg vehicle impacting at 100 km/h at 20 degrees. This compares to a model prediction here of ASI = 1.61 for this same impact configuration. As stated earlier, the twelve data points in

Table 1 reported by Anghileri, et al. (2005) are from nominally identical TB11 tests where recorded dynamic deflection is zero. The reported ASI values for these tests range from 1.27 to 1.94 with a mean of 1.55. In analysis of ASI versus dynamic deflection (DD) for 174 TB11 tests, Anghileri, et al. (2005) reported the line of best fit as $ASI = 1.4448e^{-0.683 \times DD}$ which would yield ASI = 1.44 for a rigid barrier (DD = zero) impacted under TB11 conditions. The point here though, as evidenced in Figure 3 and Table 5 is that the Equation 12 model appears to deliver a realistic value (ASI = 1.61) for the TB11 test configuration.

Conclusions and suggestions for further work

The aim of this study was to construct and then test a desktop model that would predict ASI values for impacts into rigid barriers. This has been done at Equation 12. The model has demonstrated some level of validity: CURE plots are generally well-behaved and moreover predicted values for each standardised test impact configuration correspond very well with the average observed values for each test configuration. Comparison with similar work conducted by others invites further investigation.

The model would benefit from further refinement, ideally incorporating results from full-scale crash testing in configurations other than those prescribed in the test protocols. The model may also need to be refined to take into account variations in both vehicle (e.g., stiffness) and barrier (e.g., shape, friction).

An overall conclusion of this study is that ASI appears to be a predictable function of impact mass, speed and angle. However for the purposes of practical application, the model would need to be enhanced by (for example) determination of the nature of the 'a' term at Equation 2.

Acknowledgements

The authors are grateful to Jade Hogan and Trent Lum of New South Wales Roads and Maritime Services for permission to use some of the crash test data cited in this paper.

Disclaimer

Any opinions expressed are those of the authors. The State of Queensland makes no statements, representations or warranties regarding the accuracy or usefulness of the information for any other use whatsoever. Any party using the information for any purpose does so at their own risk, and releases and indemnifies the State of Queensland against all responsibility and liability (including negligence, negligent misstatement and pure economic loss) for all expenses, losses, damages and costs incurred as a consequence of such use.

References

AASHTO. (2009). *Manual for assessing safety hardware (MASH)*. Washington, DC, USA: American Association of State Highway and Transportation Officials.

Alberson, D. C., Menges, W. L., & Haug, R. R. (2004). *TL-4 crash testing of the F411 bridge rail*. College Station, Texas, USA: Texas Transportation Institute.

Alberson, D. C., Williams, W. F., Menges, W. L., & Haug, R. R. (2004). *Testing and evaluation of the Florida Jersey safety shaped bridge rail*. College Station, Texas, USA: Texas Transportation Institute.

Anghileri, M. (2003). *ROBUST - Road Barrier Upgrade of Standards - Deliverables D.3.1 D.3.2*. Milan, Italy.

Anghileri, M., Luminari, M., & Williams, G. (2005). *ROBUST - Road Barrier Upgrade of Standards - Deliverable D.2.1. Analysis of test data from European laboratories*. Milan, Italy.

Bullard, D. L., Williams, W. F., Mendes, W. L., & Haug, R. R. (2002). *Design and evaluation of the TXDOT F411 and T77 aesthetic bridge rails*. College Station, Texas, USA: Texas Transportation Institute.

Bullard, L. D., Jr, Buth, C. E., Williams, W. F., Menges, W. L., & Schoeneman, S. K. (2001). *NCHRP Report 350 evaluation of the T501 bridge rail with soundwall*. College Station, Texas, USA: Texas Transportation Institute.

Burbridge, A., & Troutbeck, R. (2017a). Decompartmentalising road safety barrier stiffness in the context of vehicle occupant risk. *Journal of the Australasian College of Road Safety*, 28(1), 11-19.

Burbridge, A., & Troutbeck, R. (2017b). *Feasibility of predicting light vehicle occupant injury disutility from impacts with road safety barriers*. Paper presented at 1st International Roadside Safety Conference, San Francisco, CA, USA.

Buth, C. E., Bligh, R. P., & Menges, W. L. (1998). *NCHRP Report 350 test 3-11 of the Texas type T411 bridge rail*. College Station, Texas, USA: Texas Transportation Institute.

Buth, C. E., Menges, W. L., & Williams, W. F. (1999). *Testing and evaluation of the New York two-rail curbless and four-rail curbless bridge railing and the box-beam transition*. College Stattion, Texas, USA: Texas Transportation Institute.

Buth, C. E., Williams, W. F., Bligh, R. P., Menges, W. L., & Butler, B. G. (1998). *Tests 4, 5, & 6: NCHRP Report 350 testlng of the Texas type T202 bridge rail*. College Station, Texas, USA: Texas Transportation Institute.

Buth, C. E., Williams, W. F., Bligh, R. P., Menges, W. L., & Haug, R. R. (2002). *Performance of the TXDOT T202 (mod) bridge rail reinforced with fiber reinforced polymer bars*. College Station, Texas, USA: Texas Transportation Institute.

Buth, C. E., Williams, W. F., Menges, W. L., & Schoeneman, S. S. (1998). *NCHRP Report 350 test 4-10 of the Alaska multi-state bridge rail*. College Station, Texas, USA: Texas Transportation Institute.

European Committee for Standardization. (2010a). *EN 1317-1 Road Restraint Systems - Part 1: Terminology and General Criteria for Test Methods*. Brussels, Belgium: CEN.

European Committee for Standardization. (2010b). *EN 1317-2 Road Restraint Systems - Part 2: Performance Classes, Impact Test Acceptance Criteria and Test Methods for Safety Barriers including Vehicle Parapets*. Brussels, Belgium: CEN.

Federal Highway Administration. (2000). Letter ref. HSA-1\HSA-B73. Washington, DC, USA: US Department of Transportation.

Gabauer, D., & Gabler, H. C. (2005). Evaluation of the acceleration severity index threshold values utilizing event data recorder technology. *Transportation Research Record: Journal of the Transportation Research Board*, 1904(-), 37-45.

Hammonds, B. R., & Troutbeck, R. J. (2012). *Crash test outcomes for three generic barrier types*. Paper presented at 25th ARRB Conference – Shaping the future: linking research, policy and outcomes, Perth, WA, Australia.

Hauer, E. (2015). *The art of regression modeling in road safety*. Switzerland: Springer International Publishing.

Hirsch, T. J., Harris, W. J., James, R. W., Lamkin, J., & Zhang, H. (1989). *Analysis and design of metrorail-railroad barrier system*. College Station, Texas, USA: Texas Transportation Institute.

Jehu, V., & Prisk, C. W. (1967). *Research on crash barriers-their design, warrants for use, safety aspects, testing and research*. Paris, France: Organisation for Economic Co-operation and Development (OECD).

Jiang, T., Grzebieta, R. H., & Zhao, X. L. (2004). Predicting impact loads of a car crashing into a concrete roadside safety barrier. *International Journal of Crashworthiness*, 9(1), 45-63.

Li, N., Fang, H., Zhang, C., Gutowski, M., Palta, E., & Wang, Q. (2015). A numerical study of occupant responses and injuries in vehicular crashes into roadside barriers based on finite element simulations. *Advances in Engineering Software*, 90(-), 22-40.

LIER. (2006). *ROBUST - Road Barrier Upgrade of Standards - Deliverables D.4.1.1*. Milan, Italy.

Montella, A., & Pernetti, M. (2004). *Vehicle occupant impact severity in relation to real world impact conditions*. Paper presented at 2nd International Congress on New Technologies and Modeling Tools for Roads, Florence, Italy.

Naish, D. A., & Burbridge, A. (2015). Occupant severity prediction from simulation of small car impact with various concrete barrier profiles. *International Journal of Crashworthiness*, 20(5), 510-523.

Noel, J. S., Hirsch, T. J., Buth, C., & Arnold, A. (1981). Loads on bridge railings. *Transportation Research Record: Journal of the Transportation Research Board*, 796(-), 31-35.

Roque, C., & Cardoso, J. L. (2013). Observations on the relationship between European standards for safety barrier impact severity and the degree of injury sustained. *IATSS Research*, 37(1), 21-29.

Ross, H. E., Sicking, D. L., Zimmer, R. A., & Michie, J. D. (1993). *NCHRP Report 350: Recommended Procedures for the Safety Performance Evaluation of Highway Features*. Washington, DC, USA: Transportation Research Board.

Sherry, D., & Jackson, C. (2010a). *Test Report: BR2010/006 type 'F' concrete safety barrier*. Huntingwood, NSW, Australia: NSW Roads and Traffic Authority.

Sherry, D., & Jackson, C. (2010b). *Test Report: BR2010/010 type 'F' concrete safety barrier*. Huntingwood, NSW, Australia: NSW Roads and Traffic Authority.

Sherry, D., & Jackson, C. (2010c). *Test Report: BR2010/011 type 'F' concrete safety barrier*. Huntingwood, NSW, Australia: NSW Roads and Traffic Authority.

Sherry, D., & Jackson, C. (2010d). *Test Report: BR2010/013 type 'F' concrete safety barrier*. Huntingwood, NSW, Australia: NSW Roads and Traffic Authority.

Shojaati, M. (2003). *Correlation between injury risk and impact severity index ASI*. Paper presented at 3rd Swiss Transport Research Conference, Monte Verità, Ascona, Switzerland.

Speer, D., Peter, R., White, M., & Jewell, J. (2002). *Crash testing of various textured barriers*. Sacramento, CA, USA: California Department of Transportation.

Standards Australia. (2015). *AS/NZS 3845.1 Road safety barrier systems*. Strathfield, New South Wales, Australia; Wellington, New Zealand: Standards Australia; Standards New Zealand.

Sturt, R., & Fell, C. (2009). The relationship of injury risk to accident severity in impacts with roadside barriers. *International Journal of Crashworthiness*, 14(2), 165-172.

Whitesel, D., Jewell, J., & Meline, R. (2008). *Development and Crash Testing of an Aesthetic, See-Through Bridge Rail, Type 90*. Sacramento, CA, USA: California Department of Transportation.

Williams, W. F., Bligh, R. P., & Menges, W. L. (2011). *MASH test 3-11 of the TXDOT single slope bridge rail (type SSTR) on pan-formed bridge deck.* College Station, Texas, USA: Texas Transportation Institute.